
Optimal transport mapping via input convex neural networks

Ashok Vardhan Makkuva *
University of Illinois at Urbana-Champaign
makkuva2@illinois.edu

Amirhossein Taghvaei *
University of Illinois at Urbana-Champaign
amirhoseintghv@gmail.com

Sewoong Oh
University of Washington
sewoong@cs.washington.edu

Jason D. Lee
Princeton University
jasonlee@ee.princeton.edu

Abstract

In this paper, we present a novel and principled approach to learn the optimal transport between two distributions, from samples. Guided by the optimal transport theory, we learn the optimal Kantorovich potential which induces the optimal transport map. This involves learning two convex functions, by solving a novel minimax optimization. Building upon recent advances in the field of input convex neural networks, we propose a new framework where the gradient of one convex function represents the optimal transport mapping. Numerical experiments confirm that we learn the optimal transport mapping. This approach ensures that the transport mapping we find is optimal independent of how we initialize the neural networks. Further, target distributions from a discontinuous support can be easily captured, as gradient of a convex function naturally models a *discontinuous* transport mapping.

1 Introduction

Finding a mapping that transports a mass from one distribution Q to the other P has several applications. Training deep generative models to sample from a realistic distribution, relies on finding a mapping from a predefined distribution to the target distribution. This includes generative adversarial networks [GPAM⁺14], generative moment matching networks [LSZ15], minimizing maximum mean discrepancy [LCC⁺17], and variational autoencoders [KW13]. Domain adaptation requires mapping the source domain to the target domain, to align the patterns discovered in the former to the latter. Finding a natural alignment that preserves similarities is critical [GLC11, BDBC⁺10].

There are many mappings T that can map a random variable X from Q such that $T(X)$ is distributed as P . Optimal transport addresses the problem of finding one that minimizes the total cost of transporting mass from Q to P , as originally formulated in [Mon81]. Optimal mappings are useful in several applications including color transfer [FPPA14], shape matching [SWS⁺15], data assimilation [Rei13], Bayesian inference [EMM12]. For discrete variables, the optimal transport can be found as a solution to linear program. Hence, typical approaches to learn the optimal transport is based on quantization and cannot be extended to high-dimensional variables [EG99, BB00, PPO14].

We propose a novel minimax optimization to learn the optimal transport under the quadratic distance or Wasserstein-2 metric. The key innovation is to depart from the common practice of adding regularizers to eliminate the challenging constraints in the Kantorovich dual formulation (3). This regularization creates a bias that hinders learning the true optimal transport. Instead, we eliminate the constraints by restricting our search to the set of all convex functions, building upon the fundamental

*Equal Contribution. Order decided by a coin flip.

connection from Theorem 3.2. This leads to a novel minimax formulation in (6). Leveraging the recent advances in input convex neural networks, we propose an algorithm for solving this minimax optimization, and experimentally showcase its performance. From the perspective of training generative models, our approach can be viewed as a novel framework to train a generator that is modeled as a *gradient of a convex function*. We provide a principled training rule based on the optimal transport theory. This ensures that the generator converges to the optimal transport, independent of how we initialize the neural network. Further, gradient of a neural network naturally represents discontinuous functions, which is critical whenever the target distribution has a disconnected support.

To model convex functions, we leverage Input Convex Neural Networks (ICNNs), a class of scalar-valued neural networks $f(x; \theta)$ such that the function $x \mapsto f(x; \theta) \in \mathbb{R}$ is convex. These neural networks were introduced by [AXK16] to provide efficient inference and optimization procedures for structured prediction, data imputation and reinforcement learning tasks. In this paper, we show that ICNNs can be efficiently trained to learn the optimal transport map between two distributions P and Q . To the best of our knowledge, this is the first such instance where ICNNs are leveraged for the well-known task of learning optimal transport maps in a scalable fashion. This framework opens up a new realm for understanding problems in optimal transport theory using parametric convex neural networks, both in theory and practice. Figure 1 provides an example where the optimal transport map has been learned via the proposed Algorithm 1 from the orange distribution to the green distribution.

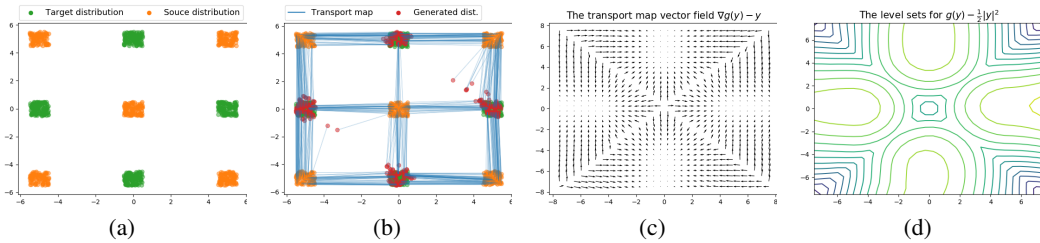


Figure 1: Checker-board example: (a) Samples from the source distribution (orange) and target distribution (green); (b) The learned transport map and the generated distribution, via Algorithm 1; (c) The learned displacement vector field generated by $\nabla g(y) - y$; (d) The level sets of the original dual variable $g(y) - \frac{1}{2}|y|^2$. The experimental details are included in Section 4.2.

Notation. δ_y denotes the Dirac distribution at y , $y \in \mathbb{R}$. Id denotes the identity function, i.e. $\text{Id}(x) = x$. For any function $F : \mathbb{R}^d \rightarrow \mathbb{R}^d$, $\text{Graph}(F) \triangleq \{(x, F(x)) : x \in \mathbb{R}^d\}$. For any two measures P, Q on \mathbb{R}^d , $P \otimes Q$ denotes their product measure on $\mathbb{R}^d \times \mathbb{R}^d$. We denote the set of all convex functions $f : \mathbb{R}^d \rightarrow \mathbb{R}$ by CVX_d . ℓ_2 -Euclidean norm is denoted by $\|\cdot\|$. f -diff. denotes that the function $f : \mathbb{R}^d \rightarrow \mathbb{R}$ is differentiable. For any measure μ , let $L^1(\mu) \triangleq \{f \text{ is measurable \& } \int f d\mu < \infty\}$.

2 Related work and background on optimal transport

For any Polish space X , let $\mathcal{P}(X)$ denote the set of all probability distributions on X , and $\mathcal{B}(X)$ denote the set of all Borel-measurable subsets of X . Let P and Q be two probability distributions on \mathbb{R}^d with finite second order moments. For any measurable mapping $T : \mathbb{R}^d \rightarrow \mathbb{R}^d$, let $T_{\#}Q$ denote the push-forward of the measure Q under T , i.e. $(T_{\#}Q)(A) = Q(T^{-1}(A))$ for all $A \in \mathcal{B}(\mathbb{R}^d)$. Let $c(x, y) = \frac{1}{2}\|x - y\|_2^2$ be the standard quadratic cost. Then the *Monge's optimal transportation problem* is to transport the probability mass under Q to P with the least quadratic cost, i.e.

$$\underset{T: T_{\#}Q=P}{\text{minimize}} \quad \frac{1}{2} \mathbb{E}_Q \|X - T(X)\|^2, \quad (1)$$

Any transport map T achieving the minimum in (1) is called the *optimal transport map*. The optimal transport maps may not exist. In fact, the feasible set in the above optimization problem may itself be empty, for example when Q is a Dirac distribution and P is any non-Dirac distribution.

To extend this notion of distance between P and Q in (1), Kantorovich considered a relaxed version in [Kan58, Kan06]. When an optimal transport map exists, the following second Wasserstein distance

recovers (1). Further, $W_2(\cdot, \cdot)$ is well-defined, even when an optimal transport map might not exist. In particular, it is defined as

$$W_2^2(P, Q) \triangleq \inf_{\pi \in \Pi(P, Q)} \frac{1}{2} \mathbb{E}_{(X, Y) \sim \pi} \|X - Y\|^2, \quad (2)$$

where $\Pi(P, Q)$ denotes the set of all joint probability distributions (or equivalently, couplings) whose first and second marginals are P and Q , respectively. Any coupling π achieving the infimum is called the *optimal coupling*. (2) is also referred to as the *primal formulation* for Wasserstein-2 distance. Kantorovich also provided a dual formulation for (2), well-known as the Kantorovich duality theorem [Vil03, Theorem 1.3], given by

$$W_2^2(P, Q) = \inf_{\pi \in \Pi(P, Q)} \frac{1}{2} \mathbb{E}_{(X, Y) \sim \pi} \|X - Y\|^2 = \sup_{(f, g) \in \Phi_c} \mathbb{E}_P[f(X)] + \mathbb{E}_Q[g(Y)], \quad (3)$$

where Φ_c denotes the constrained space of functions, defined as $\Phi_c \triangleq \{(f, g) \in L^1(P) \times L^1(Q) : f(x) + g(y) \leq \frac{1}{2} \|x - y\|_2^2, \quad \forall (x, y) dP \otimes dQ \text{ a.e.}\}$.

As there is no easy way to ensure the feasibility of the constraints along the gradient updates, common approach is to translate the optimization into a tractable form, while sacrificing the original goal of finding the optimal transport [Cut13]. Concretely, an entropic or a quadratic regularizer is added to (2). This makes the dual an unconstrained problem, which can be numerically solved using Sinkhorn algorithm [Cut13] or stochastic gradient methods [GCPB16, SDF⁺17]. The optimal transport can then be obtained from f and g , using the first-order optimality conditions of the Fenchel-Rockafellar's duality theorem.

In this paper, we take a different approach and aim to solve the dual problem, without introducing a regularization. This idea is also considered classically in [CWVB09] and more recently in [GAQ⁺19] and [TJ19]. The classical approach relies on the exact knowledge of the density, which is not available in practice. The approach in [GAQ⁺19] relies on the discrete Brenier theory which is computationally expensive and not scalable. The most related work to ours is [TJ19], which we provide a formal comparison in Section 3.

3 A novel minimax formulation to learn optimal transport

Our goal is to learn the optimal transport map T^* from Q to P , from samples drawn from P and Q , respectively. We use the fundamental connection between optimal transport and Kantorovich dual in Theorem 3.2, to formulate learning T^* as a problem of estimating $W_2^2(P, Q)$. However, $W_2^2(P, Q)$ is notoriously hard to estimate. The standard Kantorovich dual formulation in Eq. (3) involves a supremum over a set Φ_c with infinite constraints, which is challenging to even approximately project onto. To this end, we derive an alternative optimization formulation in Eq. (6), inspired by the convexification trick [Vil03, Section 2.1.2]. This allows us to eliminate the distance constraint of Φ_c , and instead constrain our search over all *convex functions*. This constrained optimization can now be seamlessly integrated with recent advances in designing deep neural architectures with convexity guarantees. This leads to a novel minimax optimization to learn the optimal transport.

We exploit the fundamental properties of $W_2^2(P, Q)$ and the corresponding optimal transport to reparametrize the optimization formulation. Note that for any $(f, g) \in \Phi_c$, we have

$$f(x) + g(y) \leq \frac{1}{2} \|x - y\|_2^2 \iff \left[\frac{1}{2} \|x\|_2^2 - f(x) \right] + \left[\frac{1}{2} \|y\|_2^2 - g(y) \right] \geq \langle x, y \rangle.$$

Hence reparametrizing $\frac{1}{2} \|\cdot\|_2^2 - f(\cdot)$ and $\frac{1}{2} \|\cdot\|_2^2 - g(\cdot)$ by f and g respectively, and substituting them in (3), the dual form modifies to

$$W_2^2(P, Q) = \frac{1}{2} \mathbb{E}_P \|X\|_2^2 + \frac{1}{2} \mathbb{E}_Q \|Y\|_2^2 - \inf_{(f, g) \in \tilde{\Phi}_c} \left\{ \mathbb{E}_P[f(X)] + \mathbb{E}_Q[g(Y)] \right\}, \quad (4)$$

where $\tilde{\Phi}_c \triangleq \{(f, g) \in L^1(P) \times L^1(Q) : f(x) + g(y) \geq \langle x, y \rangle, \quad \forall (x, y) dP \otimes dQ \text{ a.e.}\}$. While the above constrained optimization problem involves a pair of functions (f, g) , it can be transformed into the following form involving only a single convex function f , thanks to [Vil03, Theorem 2.9]:

Theorem 3.1. For any two probability distributions P and Q on \mathbb{R}^d with finite second order moments, we have that

$$\inf_{(f,g) \in \tilde{\Phi}_c} \mathbb{E}_P[f(X)] + \mathbb{E}_Q[g(Y)] = \inf_{f \in \text{CVX}(\mathbb{R}^d)} \mathbb{E}_P[f(X)] + \mathbb{E}_Q[f^*(Y)],$$

where $f^*(y) = \sup_x \langle x, y \rangle - f(x)$ is the convex conjugate of $f(\cdot)$.

This single function representation does not make the problem any less challenging, as the definition of $f^*(\cdot)$ involves solving an optimization. However, the fact that we only need to search over convex $f(\cdot)$ is surprising, which leads to the novel representation of the optimal transport as a gradient of a convex function in the following. In view of Theorem 3.1, we have from (4) that

$$W_2^2(P, Q) = \frac{1}{2} \mathbb{E}_P \|X\|_2^2 + \frac{1}{2} \mathbb{E}_Q \|Y\|_2^2 - \inf_{f \in \text{CVX}(\mathbb{R}^d)} \left\{ \mathbb{E}_P[f(X)] + \mathbb{E}_Q[f^*(Y)] \right\}. \quad (5)$$

The crucial tools behind our formulation are the following celebrated results due to Knott-Smith and Brenier [Vil03], which relate the optimal solutions for the dual form in (5) and the primal form in (2).

Theorem 3.2 ([Vil03, Theorem 2.12]). Let P, Q be any two probability distributions on \mathbb{R}^d with finite second order moments. Then,

1. (**Knott-Smith optimality criterion**) A coupling $\pi \in \Pi(P, Q)$ is optimal for the primal (2) if and only if there exists a convex function $f \in \text{CVX}(\mathbb{R}^d)$ such that $\text{Supp}(\pi) \subset \text{Graph}(\partial f)$. Or equivalently, for all $d\pi$ -almost (x, y) , $y \in \partial f(x)$. Moreover, the pair (f, f^*) achieves the minimum in the dual form (5).
2. (**Brenier's theorem**) If Q admits a density with respect to the Lebesgue measure on \mathbb{R}^d , then there is a unique optimal coupling π for the primal problem. In particular, the optimal coupling satisfies that

$$d\pi(x, y) = dQ(y) \delta_{x=\nabla f^*(y)},$$

where the convex pair (f, f^*) achieves the minimum in the dual problem (5). Equivalently, $\pi = (\nabla f^* \times \text{Id})_{\#} Q$.

3. Under the above assumptions of Brenier's theorem, ∇f^* is the unique solution to Monge transportation problem from Q to P , i.e.

$$\mathbb{E}_Q \|\nabla f^*(Y) - Y\|^2 = \inf_{T: T_{\#} Q = P} \mathbb{E}_Q \|T(Y) - Y\|^2.$$

Remark 3.3. Whenever Q admits a density, we refer to ∇f^* as the optimal transport map.

Henceforth, throughout the paper we assume that the distribution Q admits a density in \mathbb{R}^d , and discuss algorithmic implications of this assumption in Section 4.5. In view of Theorem 3.2, any optimal pair (f, f^*) from the dual formulation in (5) provides us an optimal transport map ∇f^* pushing forward Q onto P . We show in the following theorem that the conjugate function can be replaced by a minimax optimization involving two convex functions.

Theorem 3.4. Whenever Q admits a density in \mathbb{R}^d , we have that

$$W_2^2(P, Q) = C_{P, Q} - \inf_{\substack{f \in \text{CVX}_d \cap L^1(P), \\ f^* \in L^1(Q)}} \sup_{g \in \text{CVX}_d \cap L^1(Q)} \mathbb{E}_P[f(X)] + \mathbb{E}_Q[\langle Y, \nabla g(Y) \rangle - f(\nabla g(Y))],$$

where $C_{P, Q} = (1/2) \mathbb{E}[\|X\|_2^2 + \|Y\|_2^2]$ is a constant independent of (f, g) . In addition, there exists an optimal pair (f, g) achieving the infimum and supremum respectively, where ∇g is the optimal transport map pushing forward Q onto P .

Rearranging the terms in Theorem 3.4, we get

$$W_2^2(P, Q) = \sup_{\substack{f \in \text{CVX}_d \cap L^1(P), \\ f^* \in L^1(Q)}} \inf_{g \in \text{CVX}_d \cap L^1(Q)} \mathbb{E}[f(\nabla g(Y)) - f(X)] - \mathbb{E}[\langle Y, \nabla g(Y) \rangle] + C_{P, Q}, \quad (6)$$

where $(X, Y) \sim P \otimes Q$. This provides a principled approach to learn the optimal transport mapping $\nabla g(\cdot)$ as a solution of a minimax optimization.

Since the optimization formulation in (6) involves the search over the space of convex functions, we utilizing recent advances in input convex neural networks to parametrize them in Section 3.1.

3.1 Minimax optimization over input convex neural networks

We propose using parametric models based on deep neural networks to approximate the set of convex functions. This is known as input convex neural networks [AXK16], denoted by ICNN(\mathbb{R}^d). We propose estimating the following approximate Wasserstein-2 distance, from samples:

$$\widetilde{W}_2^2(P, Q) = \sup_{f \in \text{ICNN}(\mathbb{R}^d)} \inf_{g \in \text{ICNN}(\mathbb{R}^d)} \mathbb{E}[f(\nabla g(Y)) - f(X)] - \mathbb{E}[\langle Y, \nabla g(Y) \rangle] + C_{P, Q}. \quad (7)$$

Input convex neural networks (ICNNs) are a class of scalar-valued neural networks $f(x; \theta)$ such that the function $x \mapsto f(x; \theta) \in \mathbb{R}$ is convex. The neural network architecture for an ICNN is as follows. Given an input $x \in \mathbb{R}^d$, the mapping $x \mapsto f(x; \theta)$ is given by a L -layer feed-forward NN using the following equations for $l = 0, 1, \dots, L - 1$:

$$z_{l+1} = \sigma_l(W_l z_l + A_l x + b_l), \quad f(x; \theta) = z_L,$$

where $\{W_l\}$, $\{A_l\}$ are weight matrices (with the convention that $W_0 = 0$), and $\{b_l\}$ are the bias terms. σ_l denotes the entry-wise activation function at the layer l . This is illustrated in Figure 2. We denote the total set of parameters by $\theta = (\{W_l\}, \{A_l\}, \{b_l\})$. It follows from [AXK16, Proposition 1] that $f(x; \theta)$ is convex in x provided

- (i) all entries of the weights W_l are non-negative
- (ii) the activation function σ_0 is convex
- (iii) the activation function σ_l is convex and non-decreasing, for $l = 1, \dots, L - 1$.

While ICNNs are a specific parametric class of convex functions, it is important to understand if this class is rich enough representationally. This is answered positively by [CSZ18, Theorem 1]. In particular, they show that any convex function over a compact domain can be approximated in sup norm by a ICNN to the desired accuracy. This justifies the choice of ICNNs as a suitable approximating class for the convex functions.

Remark 1. The proposed framework for learning the optimal transport provides a novel training method for deep generative models, where (a) the generator is modeled as a gradient of a convex function and (b) the minimax optimization in (7) (and more concretely the update rule in Algorithm 1) provides the training rule. On the surface, Eq. (7) resembles the minimax optimization of generative adversarial networks based on Wasserstein-1 distance [ACB17], called WGAN. However, there are several critical differences making our approach attractive.

First, because WGANs use optimal transport distance only as a measure of distance, the learned transport map from the latent source to the target is arbitrary (see Figure 4) [JSA⁺18]. Hence, it is sensitive to the initialization. On the other hand, we find the *optimal* transport map and converges to the same mapping regardless of the initialization (see Figure 1). Further, this makes the training stable.

Secondly, in a WGAN architecture [ACB17, PFL17], the transport map (which is the generator) is represented with neural networks that is a continuous mapping. Although, a discontinuous map can be approximated arbitrarily close with continuous neural networks, such a construction requires large weights making training unstable. On the other hand, through our proposed method, by representing the transport map with *gradient* of the neural network (equipped with ReLU type activation functions), we obtain a naturally *discontinuous map*. As a consequence we have sharp transition from one part of the support to the other, whereas GANs (including WGANs) suffer from spurious probability masses that are not present in the target. This is illustrated in Section 4.4. The same holds for regularization-based methods for learning optimal transport [GCPB16, SDF⁺17], where transport map is parametrized by neural networks.

Remark 2. In a recent work [TJ19], ICNNs have been proposed for learning the Kantorovich dual. The main difference is that [TJ19] proposes solving a single maximization over a convex function f , and a convex optimization is proposed to find the gradient of f that involves the gradient of f^* . The conjugate needs to be computed by solving a convex optimization problem for all samples at each iteration, and is challenging to scale to large datasets. Instead, we propose a min-max formulation to learn the conjugate function in a scalable fashion.

4 Experiments

We use the following synthetic datasets, (i) Checker-board in Figure 1(a), (ii) Eight Gaussians in Figure 3(a), and (iii) Circle in Figure 3(c), to show that the proposed approach converges to a global optima and finds an optimal transport map (Section 4.2), where as other Wasserstein distance based methods converge to a local minima and find arbitrary transport maps (Section 4.3). Further, the proposed method can naturally represent the desired *discontinuous* transport maps, whereas competing approaches are restricted continuous maps, resulting in spurious probability masses (Section 4.4). We further introduce a heuristic to train our model on data in lower-dimensional manifolds to learn an optimal *stochastic* transport mappings (Section 4.5).

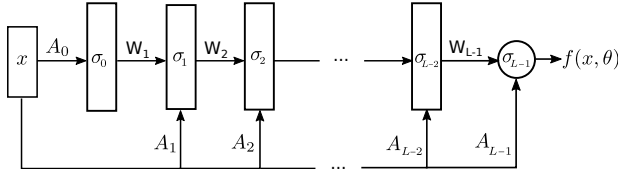


Figure 2: The input convex neural network architecture.

4.1 Experimental Setup

Neural Network Architecture: We propose ICNNs to parametrize both convex functions f and g as shown in Figure 2. Both networks have equal number of nodes for all the hidden layers followed by a final output layer. We choose a square of leaky ReLU function, i.e $\sigma_0(x) = (\max(\alpha x, x))^2$ with a small positive constant α as the *convex* activation function for the first layer σ_0 . For the remaining layers, we use the leaky ReLU function, i.e $\sigma_l(x) = \max(\alpha x, x)$ for $l = 1, \dots, L - 1$, as the *monotonically non-decreasing* and *convex* activation function. Note that this choice of activations naturally satisfy the assumptions (ii)-(iii) of the ICNN. In all of our experiments, we set the parameter $\alpha = 0.2$.

The intuition behind choosing σ_0 to be the square of the leaky ReLU function is as follows: Since the learned optimal transport map is given by ∇g , where g is an ICNN, ∇g is a piecewise constant map when the activation is just the leaky ReLU. In the case of a piecewise constant map, its gradient maps the domain of each piece to a single point. Clearly, this is not desirable as it results in generalization issues. On the other hand, using the squared version can mitigate this problem since its gradient is piecewise affine.

Optimization Procedure: The weights $\{A_l\}$ and $\{W_l\}$ are initialized with a uniform distribution on $[0, 0.1]$. The bias terms $\{b_l\}$ are initialized at zero. To ensure convexity, we need to restrict all weights W_ℓ 's to be non-negative (Assumption (i) in ICNN). We enforce it strictly for f , as a non-convex f can render the maximization over g to diverge and thus making the optimization unstable. However, for g , we relax this constraint and instead introduce a regularization term

$$R(\theta_g) = \lambda \sum_{w \in \{W_l\} \in \theta_g} (\max(-w, 0))^2,$$

where $\lambda > 0$ is the regularization constant and the summation is over all matrix components of the weight matrices $\{W_l\}$ of the network g . This relaxation makes the optimization algorithm converge faster.

For both the maximization and minimization updates in (7), we use Adam [KB14]. At each iteration, we draw a batch of samples from P and Q , denoted by $\{X_i\}_{i=1}^M$ and $\{Y_j\}_{j=1}^M$ respectively. The objective (7) thus translates to

$$\max_{\theta_f: W_\ell \geq 0, \forall \ell \in [L-1]} \min_{\theta_g} J(\theta_f, \theta_g) = \frac{1}{M} \sum_{i=1}^M f(\nabla g(Y_i)) - \langle Y_i, \nabla g(Y_i) \rangle - f(X_i) + R(\theta_g), \quad (8)$$

where θ_f, θ_g are the parameters of f and g respectively, and $W_\ell \geq 0$ is an entry-wise constraint. This is summarized in Algorithm 1. For more experimental details, please refer to Appendix B.

Algorithm 1 Algorithm to learn the optimal transport map

- 1: **Input:** Source dist. Q , Target dist. P , Batch size M , Generator iterations K , Total iterations T
 - 2: **for** $t = 1, \dots, T$ **do**
 - 3: Sample batch $\{X_i\}_{i=1}^M \sim P$
 - 4: **for** $k \in \{1, \dots, K\}$ **do**
 - 5: Sample batch $\{Y_i\}_{i=1}^M \sim Q$
 - 6: Update θ_g to minimize (8) using Adam
 - 7: **end for**
 - 8: Update θ_f to maximize (8) using Adam
 - 9: Project onto the positive orthant: $w \leftarrow \max(w, 0)$, for all $w \in \{W^l\} \in \theta_f$
 - 10: **end for**
-

4.2 Learning the optimal transport map

We now present experimental results suggesting that our proposed procedure indeed learns the optimal transport map. First, we consider the checker board example. The source distribution Q (orange) and the target distribution P (green) are illustrated in Figure 1(a). The learned optimal transport map, along with the pairs of generated and transported samples are depicted in Figure 1(b). Each line connects a sample from Q to its transported version. In order to illustrate that the learned convex function g captures the essential features of the problem, the displacement vector field $\nabla g(y) - y$ and the level sets of $g(y) - \frac{1}{2}|y|^2$ are depicted in Figure 1(c) and 1(d) respectively.

In the second experiment, we consider a mixture of eight Gaussians as depicted in Figure 3(a). The simulation parameters are same as that of checker board example except that the batch size $M = 256$. The learned optimal transport map, along with the generated samples are depicted in Figure 3(b).

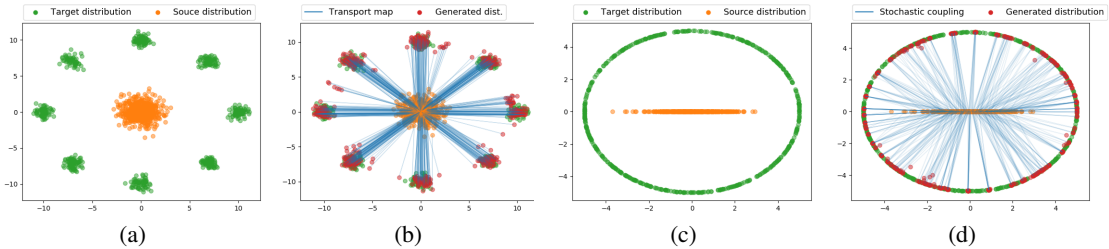


Figure 3: (a)-(b): Learning the optimal transport map for the eight Gaussians example. (a) The source and target distributions; (b) The learned transport map and the generated distribution, via Algorithm 1. (c)-(d): Learning the optimal stochastic coupling, when the optimal transport map does not exist. (c) The source and target distribution, (d) The optimal stochastic coupling and the generated distribution.

4.3 Comparisons to Wasserstein-1 GANs

We numerically show that W1-GANs find arbitrary transport maps, and hence are sensitive to initializations as discussed in Section 3. This is in stark contrast with the proposed approach which finds the optimal transport independent of how we initialize it. We consider the checker board example (Figure 1(a)) and run the state-of-the-art Wasserstein GAN introduced in [PFL17], named as W1-LP. The resulting transport map for three different random initialization are depicted in Figure 4(a), 4(b), and 4(c). In the second experiment, we considered the eight Gaussians example, and run the W1-LP algorithm [PFL17] with a batch size of $M = 64$. Figure 4(d) includes the resulting transport map.

4.4 Regularized OT methods and GANs cannot learn discontinuous transport maps

The power to represent a discontinuous transport mapping is what fundamentally sets our proposed method apart from the existing approaches, as discussed in Section 3. Two prominent approaches for learning transport maps are generative adversarial networks [ACB17, PFL17] and regularized optimal transport learning methods [GCPB16, SDF⁺17]. In both cases, the transport map is modeled

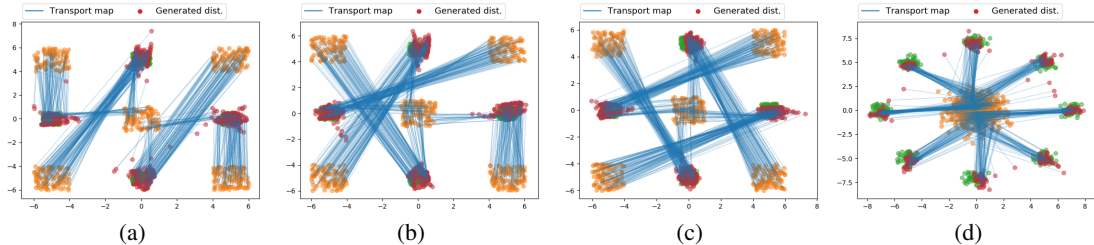


Figure 4: The learned transport map, via W1-GAN [PFL17]. (a)-(b)-(c): are for the checker board example with three different random initializations. (d) Eight Gaussians example.

by a standard neural network with finite depth and width, which is a continuous function. As a consequence, continuous transport maps suffer from unintended and undesired spurious probability mass that connects disjoint supports of the target probability distribution.

First, standard GANs including the original GAN [GPAM⁺14] and variants of WGAN [ACB17, GAA⁺17, WGL⁺18] all suffer from spurious probability masses. Even those designed to tackle such spurious probability masses, like PacGAN [LKFO18], cannot overcome the barrier of continuous neural networks. This suggests that fundamental change in the architecture, like the one we propose, is necessary. Figure 5(b) illustrates the same scenario for the transport map learned through the WGAN framework discussed in Section 4.3. We can observe the trailing dots of spurious probability masses, resulting from undesired continuity of the learned transport maps.

Similarly, regularization methods to approximate optimal transport maps, explained in Section 2, suffer from the same phenomenon. Representing a transport map with an inherently continuous function class results in spurious probability masses connecting disjoint supports. Figures 5(c) and 5(d) illustrate those trailing dots of spurious masses for the learned transport map from algorithm introduced in [SDF⁺17] with the default hyper-parameter choices, with ℓ_2 regularization and entropic regularization respectively.

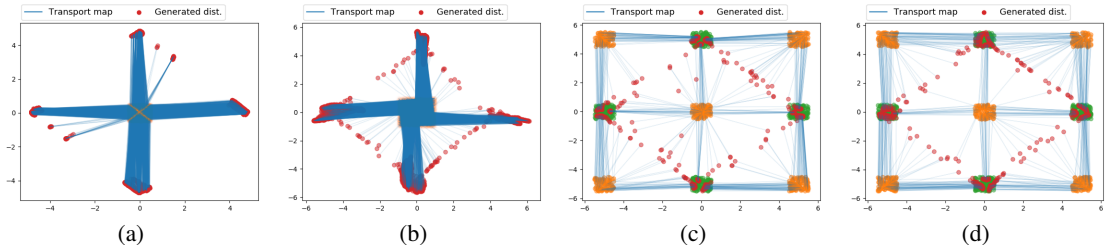


Figure 5: (a)-(b): Illustrating the discontinuous nature of the optimal transport map: (a) Our learned optimal transport map for the checker board example, evaluated only at the square located at the center; (b) The transport map learned through the W1-LP algorithm [PFL17] evaluated at the same points. (c)-(d): The regularized optimal transportation procedure [SDF⁺17] for the checker board example. (c) With ℓ_2 regularization; (d) With entropic regularization.

On the other hand, we represent the transport map with the *gradient* of a neural network (equipped with non-smooth ReLU type activation functions). The resulting transport map can naturally represent discontinuous transport maps, as illustrated in Figure 1(b) and Figure 5(a). The vector field of the learned transport map in Figure 1(c) clearly shows the discontinuity of the learned optimal transport.

4.5 Supporting low-dimensional manifolds in high-dimensions

In typical training of deep generative models, we desire to capture the low inherent dimensionality of natural distributions in high-dimensions (such as manifold of faces in high-resolution images). This is enforced by restricting the source distribution to a dimension much smaller than the ambient

dimension of the samples. We cannot directly apply our approach, as it critically relies on the fact that the source distribution admits a density, both theoretically (Remark 3.3) and in practice.

For example, consider a one dimensional Gaussian distribution as source distribution and the uniform distribution on a circle as the target distribution, as illustrated in Figure 3(c). According to the Brenier theorem, (deterministic) optimal transport map exists when at least one of the distributions admit a density. However, in this example, none of the distributions admit density.

Inspired by the Kantorovich relaxation, we propose to search for stochastic mappings instead. Recall that $Y \sim Q$ denotes the source random variable and $X \sim P$ denotes the target random variable. Define $\tilde{Y} = Y + Z$ where $Z \sim N(0, I_d)$ is a standard d -dimensional Gaussian random variable. By adding a Gaussian random variable, it follows that $\tilde{Y} \sim \tilde{Q}$ admits density. Then, we consider the optimal transport problem between \tilde{Y} and Z , which now has a deterministic optimal transport map solution. Let ∇g denote the optimal transport map. We propose the coupling induced by the stochastic map $Y \rightarrow \nabla g(Y + Z)$ as an approximation for the optimal coupling. The resulting coupling is depicted in Figure 3(d), where we learned an optimal stochastic transport map.

5 Further discussion of related work

The idea of solving the semi-dual optimization problem (5) is classically considered in [CWVB09], where the authors derive a formula for the functional derivative of the objective function with respect to f and propose to solve the optimization problem with the gradient descent method. Their approach is based on the discretization of the space and knowledge of the explicit form of the probability density functions, that is not applicable to real-world high dimensional problems.

More recently, the authors in [LSC⁺17, GAQ⁺19] propose to learn the function f in a semi-discrete setting, where one of the marginals is assumed to be a discrete distribution supported on a set of N points $\{y_1, \dots, y_N\} \subset \mathbb{R}^d$, and the other marginal is assumed to have a continuous density with compact convex support $\Omega \subset \mathbb{R}^d$. They show that the problem of learning the function f is similar to the variational formulation of the Alexandrov problem: constructing a convex polytope with prescribed face normals and volumes. Moreover, they show that, in the semi-discrete setting, the optimal f is of the form $f(x) = \max_{1 \leq i \leq N} \{\langle x, y_i \rangle + b_i\}$ and simplify the problem of learning f to the problem learning N real numbers $b_i \in \mathbb{R}$. However, the objective function involves computing polygonal partition of Ω into N convex cells, induced by the function f , which is computationally challenging. Moreover, the learned optimal transport map ∇f , transports the probability distribution from each convex cell to a single point y_i , which results in generalization issues. Additionally, the proposed approach is semi-discrete, and as a result, does not scale with the number of samples.

Statistical analysis of learning the optimal transport map through the semi-dual optimization problem (5) is studied in [HR19, RW18], where the authors establish a minimax convergence rate with respect to number of samples for certain classes of regular probability distributions. They also propose a procedure that achieves the optimal convergence rate, that involves representing the function f with span of wavelet basis functions up to a certain order, and also requiring the function f to be convex. However, they do not provide a computational algorithm to implement the procedure.

The approach proposed in this paper is built upon the recent work [TJ19], where the proposal to solve the semi-dual optimization problem (5) by representing the function f with an ICNN appeared for the first time. The proposed procedure in [TJ19] involves solving a convex optimization problem to compute the convex conjugate f^* for each sample in the batch, at each optimization iteration. This procedure becomes computationally challenging to scale to large datasets. However, in this paper, we propose a minimax formulation (6) to learn the convex conjugate function in a scalable fashion.

There are also other alternative approaches to approximate the optimal transport map that are not based on solving the semi-dual optimization problem (5). In [LSA⁺19], the authors propose to approximate the optimal transport map, through an adversarial computational procedure, by considering the dual optimization problem (3), and replacing the constraint with a quadratic penalty term. However, in contrast to the other regularization-based approaches such as [SDF⁺17], they consider a GAN architecture, and propose to take the generator, after the training is finished, as the optimal transport map. They also provide a theoretical justification for their proposal, however the theoretical justification is valid in an ideal setting where the generator has infinite capacity, the

discriminator is optimal at each update step, and the cost is equal to the exact Wasserstein distance. These ideal conditions are far from being true in a practical setting.

Another approach, proposed in [XCJ⁺19], is based on a generative learning framework to approximate the optimal coupling, instead of optimal transport map. The approach involves a low-dimensional latent random variable, two generators that take the latent variable as input and map it to a high-dimensional space where the real data resides in, and two discriminators that respectively take as inputs the real data and the output of the generator. Although, the proposed approach is attractive when an optimal transport map does not exist, it is computationally expensive because it involves learning four deep neural networks, and suffers from unused capacity issues that WGAN architecture suffers from [GAA⁺17].

Finally, a procedure is recently proposed to approximate the optimal transport map that is optimal only on a subspace projection instead of the entire space [MC19]. This approach is inspired by the sliced Wasserstein distance method to approximate the Wasserstein distance [RPDB11, DZS18]. However, selection of the subspace to project on is a non-trivial task, and optimally selecting the projection is an optimization over the Grassmann manifold which is computationally challenging.

References

- [ACB17] Martin Arjovsky, Soumith Chintala, and Léon Bottou. Wasserstein gan. *arXiv preprint arXiv:1701.07875*, 2017.
- [AXK16] Brandon Amos, Lei Xu, and J Zico Kolter. Input convex neural networks. *arXiv preprint arXiv:1609.07152*, 2016.
- [BB00] Jean-David Benamou and Yann Brenier. A computational fluid mechanics solution to the monge-kantorovich mass transfer problem. *Numerische Mathematik*, 84(3):375–393, 2000.
- [BDBC⁺10] Shai Ben-David, John Blitzer, Koby Crammer, Alex Kulesza, Fernando Pereira, and Jennifer Wortman Vaughan. A theory of learning from different domains. *Machine learning*, 79(1-2):151–175, 2010.
- [CSZ18] Yize Chen, Yuanyuan Shi, and Baosen Zhang. Optimal control via neural networks: A convex approach. *arXiv preprint arXiv:1805.11835*, 2018.
- [Cut13] Marco Cuturi. Sinkhorn distances: Lightspeed computation of optimal transport. In *Advances in neural information processing systems*, pages 2292–2300, 2013.
- [CWVB09] Rick Chartrand, Brendt Wohlberg, Kevin Vixie, and Erik Bollt. A gradient descent solution to the monge-kantorovich problem. *Applied Mathematical Sciences*, 3(22):1071–1080, 2009.
- [DZS18] Ishan Deshpande, Ziyu Zhang, and Alexander G Schwing. Generative modeling using the sliced wasserstein distance. In *Proceedings of the IEEE Conference on Computer Vision and Pattern Recognition*, pages 3483–3491, 2018.
- [EG99] Lawrence C Evans and Wilfrid Gangbo. *Differential equations methods for the Monge-Kantorovich mass transfer problem*, volume 653. American Mathematical Soc., 1999.
- [EMM12] Tarek A El Moselhy and Youssef M Marzouk. Bayesian inference with optimal maps. *Journal of Computational Physics*, 231(23):7815–7850, 2012.
- [FPPA14] Sira Ferradans, Nicolas Papadakis, Gabriel Peyré, and Jean-François Aujol. Regularized discrete optimal transport. *SIAM Journal on Imaging Sciences*, 7(3):1853–1882, 2014.
- [GAA⁺17] Ishaan Gulrajani, Faruk Ahmed, Martin Arjovsky, Vincent Dumoulin, and Aaron C Courville. Improved training of wasserstein gans. In *Advances in Neural Information Processing Systems*, pages 5767–5777, 2017.
- [GAQ⁺19] Yang Guo, Dongsheng An, Xin Qi, Zhongxuan Luo, Shing-Tung Yau, Xianfeng Gu, et al. Mode collapse and regularity of optimal transportation maps. *arXiv preprint arXiv:1902.02934*, 2019.
- [GCPB16] Aude Genevay, Marco Cuturi, Gabriel Peyré, and Francis Bach. Stochastic optimization for large-scale optimal transport. In *Advances in Neural Information Processing Systems*, pages 3440–3448, 2016.

- [GLC11] Raghuraman Gopalan, Ruonan Li, and Rama Chellappa. Domain adaptation for object recognition: An unsupervised approach. In *2011 international conference on computer vision*, pages 999–1006. IEEE, 2011.
- [GPAM⁺14] Ian Goodfellow, Jean Pouget-Abadie, Mehdi Mirza, Bing Xu, David Warde-Farley, Sherjil Ozair, Aaron Courville, and Yoshua Bengio. Generative adversarial nets. In *Advances in neural information processing systems*, pages 2672–2680, 2014.
- [HR19] Jan-Christian Hütter and Philippe Rigollet. Minimax rates of estimation for smooth optimal transport maps. *arXiv preprint arXiv:1905.05828*, 2019.
- [JSA⁺18] Leygonie Jacob, Jennifer She, Amjad Almahairi, Sai Rajeswar, and Aaron Courville. W2gan: Recovering an optimal transport map with a gan. 2018.
- [Kan58] Leonid Kantorovitch. On the translocation of masses. *Management Science*, 5(1):1–4, 1958.
- [Kan06] Leonid Vitalevich Kantorovich. On a problem of monge. *Journal of Mathematical Sciences*, 133(4):1383–1383, 2006.
- [KB14] Diederik P Kingma and Jimmy Ba. Adam: A method for stochastic optimization. *arXiv preprint arXiv:1412.6980*, 2014.
- [KW13] Diederik P Kingma and Max Welling. Auto-encoding variational bayes. *arXiv preprint arXiv:1312.6114*, 2013.
- [LCC⁺17] Chun-Liang Li, Wei-Cheng Chang, Yu Cheng, Yiming Yang, and Barnabás Póczos. Mmd gan: Towards deeper understanding of moment matching network. In *Advances in Neural Information Processing Systems*, pages 2203–2213, 2017.
- [LKFO18] Zinan Lin, Ashish Khetan, Giulia Fanti, and Sewoong Oh. Pacgan: The power of two samples in generative adversarial networks. In *Advances in Neural Information Processing Systems*, pages 1498–1507, 2018.
- [LSA⁺19] Jacob Leygonie, Jennifer She, Amjad Almahairi, Sai Rajeswar, and Aaron Courville. Adversarial computation of optimal transport maps. *arXiv preprint arXiv:1906.09691*, 2019.
- [LSC⁺17] Na Lei, Kehua Su, Li Cui, Shing-Tung Yau, and David Xianfeng Gu. A geometric view of optimal transportation and generative model. *arXiv preprint arXiv:1710.05488*, 2017.
- [LSZ15] Yujia Li, Kevin Swersky, and Richard Zemel. Generative moment matching networks. *arXiv preprint arXiv:1502.02761*, 2015.
- [MC19] Boris Muzellec and Marco Cuturi. Subspace detours: Building transport plans that are optimal on subspace projections. *arXiv preprint arXiv:1905.10099*, 2019.
- [Mon81] Gaspard Monge. Mémoire sur la théorie des déblais et des remblais. *Histoire de l'Académie royale des sciences de Paris*, 1781.
- [PFL17] Henning Petzka, Asja Fischer, and Denis Lukovnicov. On the regularization of wasserstein gans. *arXiv preprint arXiv:1709.08894*, 2017.
- [PPO14] Nicolas Papadakis, Gabriel Peyré, and Edouard Oudet. Optimal transport with proximal splitting. *SIAM Journal on Imaging Sciences*, 7(1):212–238, 2014.
- [Rei13] Sebastian Reich. A nonparametric ensemble transform method for bayesian inference. *SIAM Journal on Scientific Computing*, 35(4):A2013–A2024, 2013.
- [RPDB11] Julien Rabin, Gabriel Peyré, Julie Delon, and Marc Bernot. Wasserstein barycenter and its application to texture mixing. In *International Conference on Scale Space and Variational Methods in Computer Vision*, pages 435–446. Springer, 2011.
- [RW18] Philippe Rigollet and Jonathan Weed. Uncoupled isotonic regression via minimum wasserstein deconvolution. *arXiv preprint arXiv:1806.10648*, 2018.
- [SDF⁺17] Vivien Seguy, Bharath Bhushan Damodaran, Rémi Flamary, Nicolas Courty, Antoine Rolet, and Mathieu Blondel. Large-scale optimal transport and mapping estimation. *arXiv preprint arXiv:1711.02283*, 2017.

- [SWS⁺15] Zhengyu Su, Yalin Wang, Rui Shi, Wei Zeng, Jian Sun, Feng Luo, and Xianfeng Gu. Optimal mass transport for shape matching and comparison. *IEEE transactions on pattern analysis and machine intelligence*, 37(11):2246–2259, 2015.
- [TJ19] Amirhossein Taghvaei and Amin Jalali. 2-wasserstein approximation via restricted convex potentials with application to improved training for gans. *arXiv preprint arXiv:1902.07197*, 2019.
- [Vil03] Cédric Villani. *Topics in optimal transportation*. Number 58. American Mathematical Soc., 2003.
- [WGL⁺18] Xiang Wei, Boqing Gong, Zixia Liu, Wei Lu, and Liqiang Wang. Improving the improved training of wasserstein gans: A consistency term and its dual effect. *arXiv preprint arXiv:1803.01541*, 2018.
- [XCJ⁺19] Yujia Xie, Minshuo Chen, Haoming Jiang, Tuo Zhao, and Hongyuan Zha. On scalable and efficient computation of large scale optimal transport. *arXiv preprint arXiv:1905.00158*, 2019.

Appendix

A Proof of Theorem 3.4

Define $V_f(g) \triangleq \mathbb{E}_Q[\langle Y, \nabla g(Y) \rangle - f(\nabla g(Y))]$. The main step of the proof is to show that $\sup_{g \in \text{CVX}_d \cap L^1(Q)} V_f(g) = \mathbb{E}_Q[f^*(Y)]$. Then the conclusion follows from Theorem 3.1. To prove this, note that for all $g \in \text{CVX}_d \cap L^1(Q)$, we have

$$\langle y, \nabla g(y) \rangle - f(\nabla g(y)) \leq \langle y, \nabla f^*(y) \rangle - f(\nabla f^*(y)) = f^*(y),$$

for all $y \in \mathbb{R}^d$ such that g and f^* are differentiable at y . We now claim that both g and f^* are differentiable Q -almost everywhere (a.e). If the claim is true, upon taking the expectation w.r.t Q : $V_f(g) \leq V_f(f^*) = \mathbb{E}_Q[f^*(Y)]$, $\forall g \in \text{CVX}_d \cap L^1(Q)$ and the inequality is achieved with $g = f^*$. Hence, $\sup_{g \in \text{CVX}_d \cap L^1(Q)} V_f(g) = \mathbb{E}_Q[f^*(Y)]$. Now we prove the claim as follows: Since $\int g \, dQ < \infty$, we have $Q(g = \infty) = 0$. Thus $Q(\text{Dom}(g)) = 1$, where $\text{Dom}(g)$ is the domain of the function g . Moreover, $Q(\text{Int}(\text{Dom}(g))) = 1$, where $\text{Int}(\cdot)$ denotes the interior, because the boundary has Q -measure zero (Q has a density). Since g is convex, it is differentiable on $\text{Int}(\text{Dom}(g))$ except at points of Lebesgue measure zero which have Q -measure zero too. Therefore, g is Q -a.e differentiable. Similar arguments hold for f^* .

B Experimental set-up

For reproducibility, we provide the details of the numerical experiments.

In Section 4.2 and Figures 1(a), 1(b), 3(a), and 3(b), we run Algorithm 1 with the following parameters: The hidden size $m = 64$, number of layers $L = 4$, regularization constant $\lambda = 1.0$, batch size $M = 1024$, learning rate 10^{-4} , generator iterations $K = 10$, and the total number of iterations $T = 10^5$.

In Section 4.3 and Figures 4(a), 4(b), and 4(c), we use the state-of-the-art Wasserstein GAN introduced in [PFL17], named as W1-LP, with a fully connected neural network architecture of size $d \rightarrow m \rightarrow m \rightarrow \dots \rightarrow m \rightarrow d$ for the generator and a fully connected neural network architecture of size $d \rightarrow m \rightarrow m \rightarrow \dots \rightarrow m \rightarrow 1$ for the discriminator. The simulation parameters are as follows: the hidden size $m = 64$, number of layers $L = 4$, learning rate 10^{-4} , batch size $M = 1024$, generator iterations $K = 5$, and total number of iterations $T = 10^5$. The algorithm in [PFL17] includes a regularization constant which is chosen to be 1.0. The resulting transport map for three different random initialization are depicted in Figure 4(a), 4(b), and 4(c).

In Section 4.4 and Figures 5(c) and 5(d), we run the algorithm introduced in [SDF⁺17] with the following parameters: number of samples 512, batch size 50, entropic regularization value 0.1, l_2 regularization value 0.02, first step learning rate 5×10^{-4} , second step learning rate 2×10^{-6} , first step epochs 1000, second step epochs 100, neural network size $d \rightarrow 128 \rightarrow 256 \rightarrow 128 \rightarrow d$. These are the default values reported in [SDF⁺17]. We implemented the step one in discrete setting, because the continuous setting led to numerical instabilities. Also, decreasing the regularization parameter results in same numerical issues.

In Section 4.5 and Figures 3(c) and 3(d), we carry out the proposed procedure for the circle example in Figure 3(c). The simulation parameters are as follows: hidden layer size $m = 32$, number of layers $L = 3$, batch size $M = 256$, learning rate 10^{-4} , regularization constant $\lambda = 1.0$, generator iterations $K = 10$, total iterations $T = 10^5$. The resulting coupling is depicted in Figure 3(d).